

Kochi Chapter

Indian Geotechnical Conference  
IGC 2022  
15<sup>th</sup> – 17<sup>th</sup> December, 2022, Kochi

# Kriging-Based Approach for Reliability Analysis of Reinforced Anchors for Transmission Tower Foundations

Sougata Mukherjee<sup>1[0000-0001-5671-8714]</sup>, Rajarshi Pramanik<sup>1[0000-0002-0881-8136]</sup> and G. L. Sivakumar Babu<sup>1[0000-0002-1873-6388]</sup>

<sup>1</sup>Department of Civil Engineering, Indian Institute of Science, Bengaluru, Karnataka-560012, India

E-Mail: msougata@iisc.ac.in (S. Mukherjee), rajarshi.juconst@gmail.com (R. Pramanik), gls@iisc.ac.in (G. L. Sivakumar Babu)

**Abstract.** A reliability-based design and analysis of reinforced anchors for transmission tower foundations are presented using the Kriging-based response surface method. The improvement of the uplift capacity of anchors in reinforced soil is demonstrated using a three-dimensional numerical model. The initial design of the anchor plate is based on the uplift forces exerted at the foundation base of a typical tower subjected to lateral wind forces. Next, a Kriging metamodel is constructed to predict the uplift capacity of anchors in both unreinforced and reinforced soils to conduct reliability-based analysis considering the random nature of the uplift load, soil properties, and reinforcement stiffness. The mean uplift capacity of the anchor at 15% uplift displacement is increased by 1.35 times in the presence of reinforcement on the top of the foundation. The probabilistic analysis results indicate that the failure probability of the foundation in reinforced soil reduces significantly for the uplift forces obtained at the transmission tower foundation level. The influence of the variability of different load and resistance parameters on the stability of the foundation is examined. The variation of the reliability index with the factor of safety is presented, and the limitations of the conventional safety factor approach are discussed.

**Keywords:** Reliability Analysis, Reinforced Anchor, Numerical Modelling, Transmission Tower, Uplift Capacity, Kriging, Response Surface.

## 1 Introduction

Anchor foundations are employed under structures where the foundations are expected to resist uplift forces during their operational period. The uplift capacity of horizontal anchors has been investigated extensively both in unreinforced and reinforced soil. The significant developments in the theory of anchor uplift capacity can be found in [1–3], among others. The improvement in the pullout capacity of anchors buried under reinforcement has been investigated recently by [4, 5]. However, most of the previous studies focus on the deterministic evaluation of the anchor uplift capacity in unreinforced

and reinforced soil. Although a few studies [6–8] have reported reliability-based analysis of anchor foundations, these papers correspond to the anchor uplift capacity in unreinforced soil. The improvement of the anchor uplift capacity in reinforced soil has not been evaluated using the probabilistic framework. It has been established now that the estimation of soil properties is always prone to statistical uncertainties. Even the wind loads that generate the uplift forces on transmission towers are variable quantities that should be modelled using proper statistical models. Moreover, the conventional deterministic factor of safety (FOS) approach does not ensure adequate protection to important structures such as transmission towers, windmills etc., as the single FOS fails to address the randomness in the anchor capacity. Therefore, it is essential to incorporate the inherent variabilities in the soil and reinforcement properties (resistance) and the wind load (demand) parameters to investigate the reliability of a reinforced anchor foundation.

The probabilistic analysis of structures often requires a large number of datasets to model the performance functions where the desired output quantities cannot be expressed explicitly in analytical forms. The numerical modelling methods are used in these situations to model the physical system using different methods such as finite element (FE) or finite difference (FD) technique. The use of numerical models facilitates the study of any complex engineering problems using suitable models and assumptions. However, the simulation-based probabilistic analysis methods such as the Monte Carlo simulations (MCS) require a large number of simulations (often in the range of  $10^5$  to  $10^6$ ) to estimate the failure probability of the system. Conducting many such simulations becomes very time-consuming for three-dimensional numerical models. This problem can be solved by taking advantage of the response surface method (RSM), which uses meta models to predict the performance function numerically. Several meta modelling techniques can be used to construct the prediction model using a small number of deterministic simulation results. The constructed prediction model then can be used in the probabilistic analysis, thereby reducing the number of required deterministic simulation calls.

This paper uses the Kriging response surface model using the deterministic outputs of anchor uplift capacity in unreinforced and geogrid reinforced sand. The deterministic models are developed using the three-dimensional FD program FLAC 3D (Fast Lagrangian Analysis of Continua in 3D). The safety and reliability of a typical transmission tower foundation against uplift forces arising from lateral wind thrust acting on the tower are analysed in this study using the First Order Reliability Method (FORM). The main objectives of this study are: (i) to design and analyse reinforced anchors for application as transmission tower foundations, (ii) to implement the Kriging response surface model in the analysis of reinforced anchor uplift capacity, and (iii) to analyse the safety of reinforced anchor against varying uplift forces using the reliability-based framework that incorporates the inherent variabilities in the soil and wind properties.

## **2 Kriging-Based RSM**

In this section, a brief overview of the Kriging metamodeling is presented. In this technique, the output  $[y(\mathbf{x})]$  can be expressed as a regression model and stochastic process as below:

$$y(\mathbf{x}) = f(\mathbf{x}) + z(\mathbf{x}) \quad (1)$$

where  $f(\mathbf{x})$  is the trend function obtained by regression analysis and  $z(\mathbf{x})$  is the random error function representing the prediction error. The trend function is represented by the low-order polynomial function. In this study, the constant trend function, i.e., ordinary Kriging, is used for its capability of high-precision prediction [9]. Therefore,  $f(\mathbf{x}) = a_0$ , where  $a_0$  is the regression coefficient. The error function is considered as a stationary Gaussian process with zero mean and covariance, as shown below:

$$\text{Cov}(z(\mathbf{x}_i), z(\mathbf{x}_j)) = \sigma_z^2 R_\theta(\mathbf{x}_i, \mathbf{x}_j) \quad (2)$$

where  $\sigma_z^2$  is the process variance and  $R_\theta$  is the correlation function between two design variables  $x_i$  and  $x_j$ . In this paper, the Gaussian correlation function is used due to its advantages, as discussed by Li and Yang [9], which is expressed as

$$R_\theta(\mathbf{x}_i, \mathbf{x}_j) = \prod_{k=1}^n R_\theta(x_i^k, x_j^k, \theta_k) = \prod_{k=1}^n \exp\left[-\theta_k (x_i^k - x_j^k)^2\right] \quad (3)$$

where  $\theta_k$ ,  $k = 1, 2, \dots, n$  is the hyperparameter, and  $n$  is the total number of design variables. It is essential to find the optimal value of  $\theta_k$  for the satisfactory performance of the developed Kriging metamodel, and maximum likelihood estimator (MLE) is adopted for this purpose.

Suppose  $\mathbf{X} = [\mathbf{x}_1, \mathbf{x}_2, \dots, \mathbf{x}_m]^T$  for  $m$  sample points is the set of input variables and  $\mathbf{Y} = [y_1, y_2, \dots, y_m]^T$  is the corresponding response vector, then the unknown parameters  $a_0$  and  $\sigma_z^2$  can be obtained as below [9]:

$$\hat{\alpha}_0 = (\mathbf{1}^T \mathbf{R}^{-1} \mathbf{1})^{-1} \mathbf{1}^T \mathbf{R}^{-1} \mathbf{Y} \quad (4)$$

$$\hat{\sigma}_z^2 = \frac{1}{m} (\mathbf{Y} - \hat{\alpha}_0 \mathbf{1})^T \mathbf{R}^{-1} (\mathbf{Y} - \hat{\alpha}_0 \mathbf{1}) \quad (5)$$

where  $\mathbf{1}$  is the  $m$  dimensional column vector with all entries being 1, and  $\mathbf{R}$  is the correlation matrix including correlation functions  $R_\theta$ , which can be described as

$$\mathbf{R} = \begin{bmatrix} R_\theta(x_1, x_1) & R_\theta(x_1, x_2) & \cdot & R_\theta(x_1, x_m) \\ R_\theta(x_2, x_1) & R_\theta(x_2, x_2) & \cdot & \cdot \\ \cdot & \cdot & \cdot & \cdot \\ R_\theta(x_m, x_1) & \cdot & \cdot & R_\theta(x_m, x_m) \end{bmatrix} \quad (6)$$

So, the design response(s) can be determined using the new set of design variables  $\mathbf{x}$  using the developed model as below:

$$\hat{y}(\mathbf{x}) = \hat{\alpha}_0 + \mathbf{r}^T(\mathbf{x}) \mathbf{R}^{-1} (\mathbf{Y} - \hat{\alpha}_0 \mathbf{1}) \quad (7)$$

where  $\mathbf{r}(\mathbf{x})$  is the correlations between new set of design points  $\mathbf{x}$  and all previously used points, which can be given by,

$$\mathbf{r}(\mathbf{x}) = \{R_\theta(x, x_1), R_\theta(x, x_2), \dots, R_\theta(x, x_m)\}^T \quad (8)$$

In the present study, the Kriging method is implemented using the MATLAB toolbox DACE developed by Lophaven et al. [10].

### 3 Numerical Models

#### 3.1 Model of Transmission Tower

To obtain the forces exerted on a transmission tower foundation under wind thrust acting on the superstructure, a typical 28 m high trussed tower, having a base width of 5 m at the ground level, has been modelled in the STAAD Pro software, which is shown in Fig. 1. The Indian angle sections ISA 150×150×12 were used as members of the tower. A basic wind speed of  $V_b=50$  m/s was applied along the positive Z direction, and the wind load was modelled as per ASCE 7-10 [11] and the Guidelines for Electrical Transmission Line Structural Loading [12]. The parameters used in the wind load modelling are presented in Table 1. The forces being exerted on the tower foundations due to the resultant actions of the self-weight of the tower and the wind thrust are shown in Table 2. The vertical forces on foundations 1 and 2 are uplifting, while foundations 3 and 4 experience vertically compressive forces. The negative signs in Table 2 indicate forces along the negative axes' directions. This difference in the direction of the resultant forces is created by the overturning effect of the wind thrust, which creates tension on the windward side and compression on the leeward side. The uplift loads acting on foundations 1 and 2 were evaluated to be 245 kN.

#### 3.2 Model for Reinforced Anchor

The schematic diagram of the reinforced anchor is shown in Fig. 2. A square anchor plate of width B is embedded in reinforced soil at an embedment depth of H. The reinforcement of width b is placed on top of the anchor plate.

The anchor foundation used in this study is modelled in FLAC 3D, an explicit finite difference program containing several built-in constitutive models and structural elements. The soil medium is simulated as an elastic perfectly plastic material obeying Mohr-Coulomb failure criteria. The Liner structural element is used to simulate the anchor plate. The soil reinforcement used in this study is modelled using the built-in Geogrid structural element.

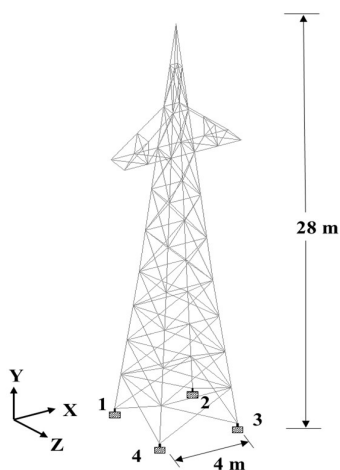


Fig 1. Numerical model of transmission tower and foundation numbers

**Table 1.** Parameters used in tower design

| Parameters                | Description                      | Values         |
|---------------------------|----------------------------------|----------------|
| H (m)                     | Height                           | 28             |
| B (m)                     | Width at ground level            | 5              |
| $V_b$ (m/s)               | Basic wind speed                 | 40             |
| Exposure                  | Exposure category                | C              |
| Risk Cat                  | Building risk category           | II             |
| Solidity ratio            |                                  | 0.2            |
| G                         | Gust response factor             | 0.88           |
| $C_f$                     | Force coefficient                | 3.06           |
| $K_z$                     | Velocity pressure exposure Coeff | 0.97           |
| $K_{zt}$                  | Topographic factor               | 1              |
| $K_d$                     | Wind directionality factor       | 0.85           |
| Structure nat. freq. (Hz) |                                  | 3              |
| Structure damping ratio   |                                  | 0.04           |
| Section                   |                                  | ISA 150×150×12 |

**Table 2.** Forces exerted on the tower foundations

| Foundation Number | Self-weight of tower (kN) |        |       | Due to wind force (kN) |        |       | Resultant $F_y$ (kN) |
|-------------------|---------------------------|--------|-------|------------------------|--------|-------|----------------------|
|                   | $F_x$                     | $F_y$  | $F_z$ | $F_x$                  | $F_y$  | $F_z$ |                      |
| 1                 | -9.47                     | -46.66 | -9.47 | -9.47                  | -46.66 | -9.47 | 245.32               |
| 2                 | 9.47                      | -46.66 | -9.47 | 9.47                   | -46.66 | -9.47 | 245.32               |
| 3                 | 9.47                      | -46.66 | 9.47  | 9.47                   | -46.66 | 9.47  | -338.64              |
| 4                 | -9.47                     | -46.66 | 9.47  | -9.47                  | -46.66 | 9.47  | -338.64              |

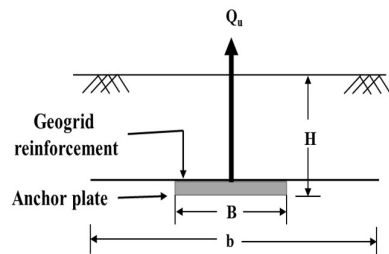


**Fig 2.** Schematic diagram of the reinforced anchor

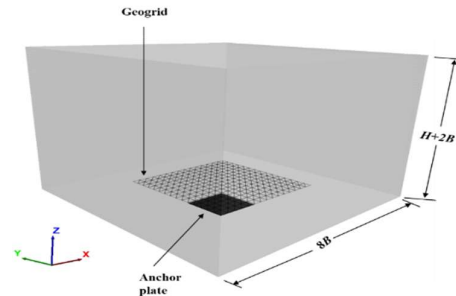


**Fig 3.** Numerical model of the reinforced anchor

### 3.3 Validation of the Numerical Model

Before the actual design and analysis of the tower foundation, the numerical model for the anchor is validated by comparing numerical results with published experimental results on unreinforced and reinforced anchors. The experimental results on single and group anchors buried in geogrid reinforced sand reported by Choudhary et al. [4] are used for validation.

A typical numerical model for the reinforced anchor is shown in Fig. 3. The sand, anchor and reinforcement properties used in these experiments are listed in Table 3.

**Table 3.** Anchor, soil, and geogrid properties used for validation

| Parameters                              | Values |
|---|--------|
| <b>Anchor properties</b>                |        |
| Width of plate, $B$ (m)                 | 0.075  |
| Depth of plate                          | 4B     |
| <b>Soil properties</b>                  |        |
| Cohesion (kPa)                          | 0      |
| Friction angle ( $^{\circ}$ )           | 37     |
| Dilation angle ( $^{\circ}$ )           | 0      |
| Unit weight ( $\text{kN/m}^3$ )         | 16.36  |
| Bulk modulus (MPa)                      | 8.33   |
| shear modulus (MPa)                     | 3.84   |
| <b>Geogrid properties</b>               |        |
| Stiffness (MPa)                         | 552    |
| Poisson's ratio                         | 0.33   |
| Interface shear modulus (MPa/m)         | 2.36   |
| Interface friction angle ( $^{\circ}$ ) | 15     |
| Interface cohesion (kPa)                | 0      |

The same properties have been used in the numerical simulations for validation. Steel anchor plates of 75 mm width ( $B$ ) and extruded biaxial geogrids with tensile stiffness of  $E_g = 550$  MPa were used in the experiments. The clear spacing ( $s$ ) between two anchors used in the experiments was  $3.4B$ . The configuration of the anchor and reinforcement used by Choudhary et al. [4] is shown in Fig. 4. The reinforcement used for group of two anchors had a length ( $l$ ) of  $9.4B$  and width ( $b$ ) of  $5B$ . The reinforcement size was symmetrically reduced to  $(b \times l/2)$  for isolated anchor and increased to  $(2b \times l)$  for a group of four anchors. The reinforcement sizes used in the experiments and the numerical simulations for different anchor configurations are indicated in Fig. 4. Fig. 5 shows the comparison between the experimental and numerical load versus displacement plots which exhibits good agreement between the experimental and numerical results in both unreinforced and reinforced sand. Therefore, it can be concluded that the present numerical model can simulate the anchor uplift behaviour both in unreinforced and reinforced soil.

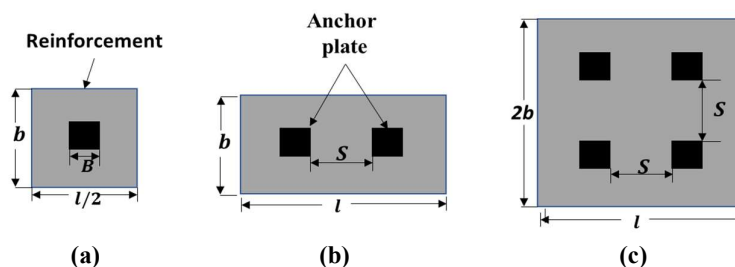


**Fig. 4.** Anchor and reinforcement configuration used in experiments by Choudhary et al. (2019a)  
**(a)** Single anchor **(b)** Group of 2 anchors **(c)** Group of 4 anchors.

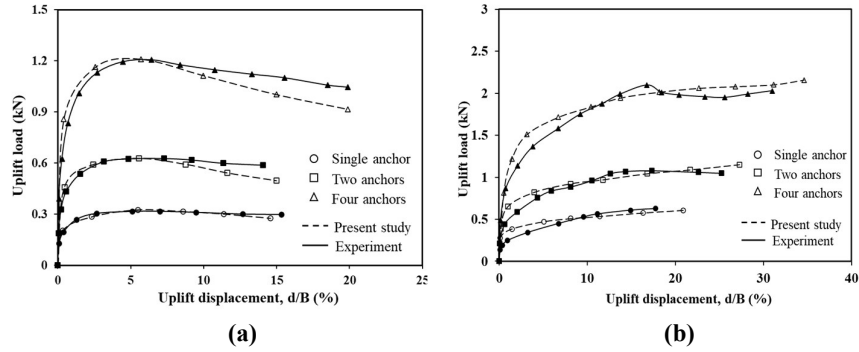


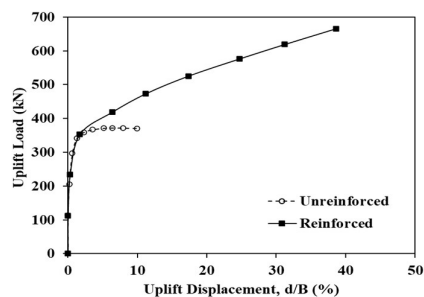
Fig 5. Validation of anchor uplift behaviour (a) unreinforced anchor (b) reinforced anchor

#### 4 Numerical Analysis and Deterministic Design of Tower Foundation

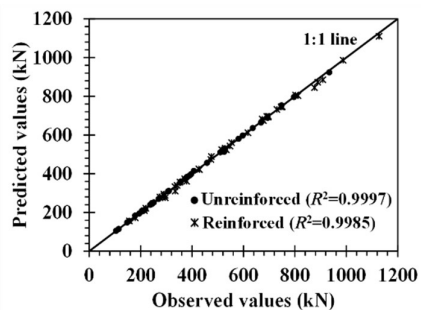
After validating the numerical model in unreinforced and reinforced sand, numerical analyses were carried out for the present study using anchors in cohesive frictional soil. First, an anchor foundation is designed in unreinforced soil to resist the uplift forces evaluated for the transmission tower foundation using a factor of safety value of 1.5 [13]. The soil properties used in the numerical analysis for the design are presented in Table 4. The shear strength properties assumed in the study are cohesion  $c=20$  kPa and internal friction angle  $\phi=30^\circ$ . A square anchor of width  $B=1$  m was found to have an uplift capacity of 372 kN at an embedment depth of  $D=2$  m. The same model was run with a layer of geogrid reinforcement having tensile stiffness  $E_g=1000$  kN/m and a width of  $3B$ , placed above the anchor plate. The comparison between the uplift load versus displacements is plotted in Fig. 6. In reinforced soil, the foundation achieves an uplift capacity of 460 kN at an uplift displacement of 10%. Whereas in unreinforced soil, the maximum uplift capacity of the anchor plate is 372 kN. Therefore, the uplift capacity improves by approximately 1.36 times in the presence of geogrid reinforcement at 15% uplift displacement. It should be noted that a massive increase (about 1.78 times) in the uplift capacity was observed at a large displacement of around 40%.

Table 4. Soil and geogrid properties for deterministic numerical model

| Properties                            | Values |
|---------------------------------------|--------|
| <b>Soil Properties</b>                |        |
| Cohesion (kPa)                        | 20     |
| Friction angle ( $^\circ$ )           | 30     |
| Unit weight ( $\text{kN/m}^3$ )       | 18     |
| Elastic Modulus (MPa)                 | 45     |
| Poisson's ratio ( $\nu_s$ )           | 0.3    |
| <b>Geogrid Properties</b>             |        |
| Geogrid Stiffness ( $J$ ) (kN/m)      | 1000   |
| Poisson's ratio ( $\nu_g$ )           | 0.33   |
| Interface shear modulus (MPa/m)       | 2.36   |
| Interface friction angle ( $^\circ$ ) | 21.14  |
| Interface cohesion (kPa)              | 13.4   |
| Depth of foundation (m)               | 2      |



**Fig 6.** Comparison of uplift load versus displacement between unreinforced and reinforced anchor



**Fig 7.** Predicted versus observed uplift forces of anchor plates

## 5 Probabilistic Analysis of Anchor Uplift Capacity

After the deterministic analysis, a probabilistic study is conducted considering random soil and geogrid properties. The mean and COV (coefficient of variation) values selected for the soil and geogrid are presented in Table 5. The uplift force acting on the foundation produced by the wind load is assumed to be a random variable with a distribution of Extreme value type-I (Gumbel distribution) [6, 12]. A mean value of 245 kN (from the initial load calculations) and  $COV=0.3-0.5$  [6] are adopted for the wind load properties.

The deterministic numerical model takes around 76 minutes to run a simulation of the reinforced anchor up to 15% displacement at a depth of 2 m. Therefore, conducting MCS using the numerical model is highly time-consuming. To reduce the computation time, a Kriging model was developed to predict the anchor's uplift capacity.

### 5.1 Performance of the Developed Kriging Model

The performance of the developed Kriging model is assessed through the coefficient of determination ( $R^2$ ) values of testing datasets for both unreinforced and reinforced anchors. Fig. 7 presents the performance of the Kriging model in predicting the uplift capacity of anchors indicating the  $R^2$  values for unreinforced and reinforced anchors.  $R^2$  values indicate the interpretation of the dependent variable by the independent variables.  $R^2$  values for unreinforced and reinforced anchors are 0.9997 and 0.9985, respectively, which confirms the accuracy and feasibility of the developed Kriging-based RSM in predicting the anchor uplift capacity.

The development of the Kriging model consists of two steps for each unreinforced and reinforced cases (i) calibration of the model and (ii) testing of the model. 105 and 42 datasets were generated for calibration and testing purposes using the Latin Hypercube Sampling (LHS) technique. The range of the random variables considered in the LHC was  $\mu \pm 3\sigma$  for each random variable considered in the design. The depth of the anchor was also varied from 1 m to 3 m with an interval of 0.1 m to incorporate the anchor depth as a design variable in the response surface.



**Table 5.** Statistical properties of soil and geogrid used in analysis

| Parameters                    | Unit              | Mean Values | COV (%) | Min<br>( $\mu-3\sigma$ ) | Max<br>( $\mu+3\sigma$ ) |
|-------------------------------|-------------------|-------------|---------|--------------------------|--------------------------|
| Soil cohesion ( $c$ )         | kPa               | 20          | 20      | 8                        | 32                       |
| Soil friction ( $\phi$ )      | Degree            | 30          | 10      | 21                       | 39                       |
| Soil unit weight ( $\gamma$ ) | kN/m <sup>3</sup> | 18          | 10      | 12.6                     | 23.4                     |
| Geogrid stiffness ( $E_g$ )   | kN/m              | 1000        | 10      | 700                      | 1300                     |

The results of the reliability analyses are presented in the form of the reliability index ( $\beta$ ), which is the shortest distance of the failure surface from the origin in an uncorrelated standard normal space of the design variables. For calculation of the reliability index ( $\beta$ ), readers are referred to [14]. A higher value of  $\beta$  indicates lower failure probability as the probability of failure can be calculated using the relation:  $P_f = \Phi(-\beta)$ , where  $\Phi$  is the cumulative distribution function (CDF) of standard normal variate.

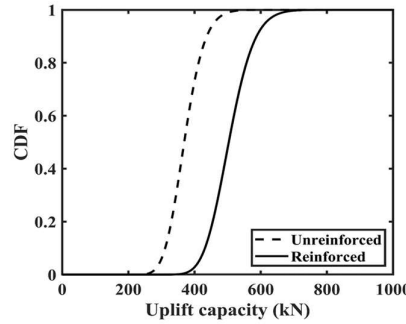


**Fig 8.** Comparison of CDF of uplift capacity between unreinforced and reinforced anchors

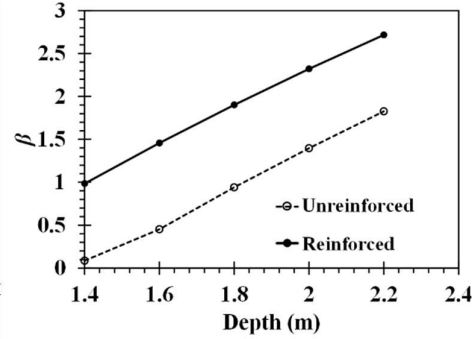


**Fig 9.** Influence of reinforcement on reliability index

## 6 Results from the Reliability-Based Study

The CDF of the anchor uplift capacity at 2 m depth was obtained using the Kriging model, assuming the statistical properties presented in Table 4 are shown in Fig. 8. The mean uplift capacities evaluated using the Kriging model are 372 kN and 506 kN for unreinforced and reinforced cases, respectively. The variation of  $\beta$  with the depth of foundation is plotted in Fig. 9. The comparison between unreinforced and reinforced cases shows increased safety from the higher reliability index of the foundation in reinforced soil. For example, the reinforced anchor achieves  $\beta=2.32$  in reinforced soil and  $\beta=1.3$  in unreinforced soil at the same depth of 2m.

Next, the influence of the variability of the random variables on the reliability index is examined by changing the COV of one variable at a time and keeping the COV of others fixed at the reference values (Table 4). First, the influence of the uplift force is presented in Fig. 10. By increasing the COV of the uplift load from 30% to 50%, the

reliability index reduces in both unreinforced and reinforced soil. This reduction is caused by the increased variability of the wind load, which increases the failure probability of the foundation. The influence of the resistance parameters on the reliability of the foundation is plotted in Fig. 11. The cohesion ( $c$ ) is found to have the most pronounced effect on  $\beta$  due to the variation of the shear strength along the failure surface. The friction angle ( $\phi$ ) and the reinforcement stiffness ( $E_g$ ) were found to have negligible effects when these two variables' COV varied from 2.5% to 10%. This minor variation in  $\beta$  due to the variation of COV in  $E_g$  is because the uplift capacity of the reinforced foundation does not change significantly when the geogrid stiffness is varied within a range of  $\mu \pm 3\sigma$ . As the unit weight of the soil ( $\gamma$ ) has a significant contribution to the weight of the soil, which is sheared and lifted upwards during failure,  $\gamma$  is also found to have a considerable contribution to the reliability of the foundation.

The design guidelines, such as [13], recommend using a FOS value of 1.5 for the uplift capacity of the foundation without considering the variabilities in the soil properties and the wind load. The wind load, being a physical phenomenon, is highly variable and can be mathematically modelled using only proper probabilistic distributions.

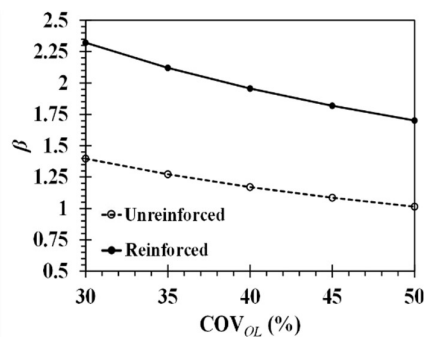


**Fig 10.** Influence of COV of uplift load on reliability index

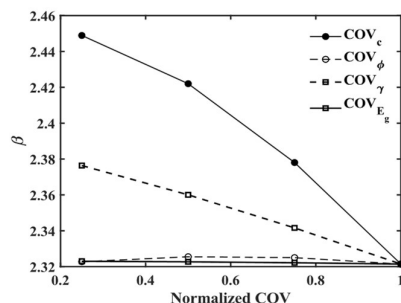


**Fig 11.** Influence of COV of resistance variables on reliability index

Besides, the FOS required for a foundation for a certain level of reliability also depends upon the properties of the design parameters involved. For this reason, a fixed FOS should not be used without proper analysis of the problem, as the required FOS will change if the statistical inputs of any design variable are altered. The variation of  $\beta$  with applied FOS is investigated by applying different FOS values to the mean uplift capacities of the unreinforced and reinforced anchors and then determining the  $\beta$  achieved in the design. The results from this investigation are presented in Fig. 12. As expected, the reliability index increases with an increase in the FOS value. However, it should be noted that the reliability indices for  $COV_{QL}=50\%$  are always lower than those for  $COV_{QL}=30\%$  for the same value of FOS in both unreinforced and reinforced soil. Usually, a target  $\beta = 2$  to 3 is recommended for the design of foundations [14]. For the codes specified  $FOS=1.5$ , the reliability indices are 1.35 and 1.37 in unreinforced and reinforced soil, respectively, when a COV value of 30% is considered for the wind load. This value is much lower than the recommended target reliability index. The required FOS values for a target  $\beta = 3$  are approximately 2.6 and 3 for 30% and 50% COV of the uplift load, respectively. Therefore, it is evident from the results that the code

specified FOS=1.5 does not ensure the required safety of the foundations. More importantly, the required FOS for the same level of reliability changes with the COV of the wind load.

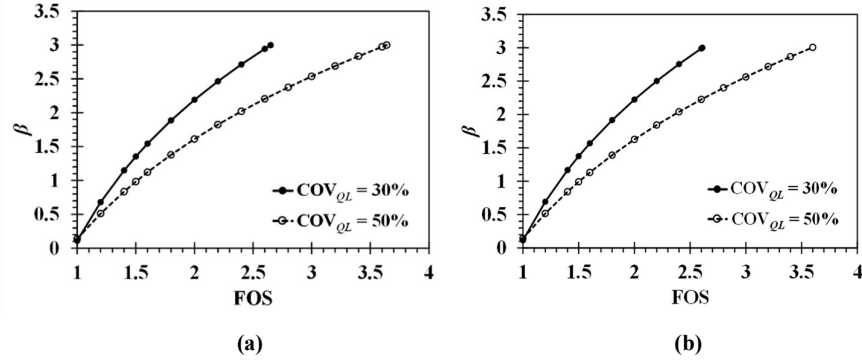


Fig 12. Variation of  $\beta$  with FOS: (a) Unreinforced (b) Reinforced anchor

## 7 Summary and Conclusions

The application of reinforced anchors for transmission towers is presented in this paper. Initially, the depth and width of an anchor are calculated for a transmission tower subjected to lateral wind thrust. Next, the improvement in the uplift capacity in the presence of geogrid reinforcement is discussed. Finally, a probabilistic study is conducted to analyse the influence of the design parameters' randomness on the foundation's safety using the Kriging surrogate model. The following conclusions can be drawn based on the findings of the study:

- (i) An improvement factor of 1.38 times was observed in the uplift capacity of the anchor when buried below a layer of geogrid reinforcement of width  $3B$ .
- (ii) A minimum  $R^2$  value of 0.99 is obtained in the calibration of the Kriging model for the prediction of the uplift capacity of unreinforced and reinforced anchors, which indicates the accuracy and efficiency of the Kriging-based surrogate model.
- (iii) The probabilistic analysis reveals that the reliability index increases for the same depth of 2 m from 1.37 to 2.32 when geogrid reinforcement is used above the anchor.
- (iv) The reliability index reduces from 1.4 to 1.01 in unreinforced soil when the COV value of the uplift load increases from 30% to 50%. A similar increase is also observed in the case of reinforced soil.
- (v) The results from the sensitivity analysis indicate that cohesion is the most sensitive parameter having the most substantial influence on the uplift capacity. In contrast, the friction angle and the reinforcement stiffness have the least significant impact.
- (vi) The required FOS for a target reliability index is found to be influenced by the COV value of the uplift load. For a target  $\beta = 3$ , the required FOS is 3, and the reliability index is approximately 1.35 for a FOS=1.5 when  $COV_{QL}=30\%$  is considered.

## Acknowledgement

The authors gratefully acknowledge the financial supports provided to the third author by Central Power Research Institute, Bengaluru (file number: CPRI0007) and to the second author by DST-SERB, India under the National Post-Doctoral Fellowship (NPDF) scheme of file number: PDF/2020/000685 at the Department of Civil Engineering, Indian Institute of Science, Bengaluru.

## References

1. Meyerhof GG, Adams JI (1968) The Ultimate Uplift Capacity of Foundations. *Canadian Geotechnical Journal* 5:225–244. <https://doi.org/10.1139/t68-024>
2. Murray EJ, Geddes JD (1987) Uplift of anchor plates in sand. *Journal of Geotechnical Engineering* 113:202–215. [https://doi.org/10.1061/\(ASCE\)0733-9410\(1987\)113:3\(202\)](https://doi.org/10.1061/(ASCE)0733-9410(1987)113:3(202))
3. Kulhawy FH., Trautman CH, Beech JF, et al (1983) *Transmission Line Structure Foundations for Uplift-Compression Loading*. Palo Alto, California
4. Choudhary AK, Pandit B, Sivakumar Babu GL (2019) Experimental and numerical study on square anchor plate groups in geogrid reinforced sand. *Geosynthetics International* 26:657–671. <https://doi.org/10.1680/jgein.19.00051>
5. Mukherjee S, Kumar L, Choudhary AK, Babu GLS (2021) Pullout resistance of inclined anchors embedded in geogrid reinforced sand. *Geotextiles and Geomembranes* 49:1368–1379. <https://doi.org/10.1016/j.geotextmem.2021.05.009>
6. Phoon K-K, Kulhawy FH, Grigoriu MD (2003) Multiple Resistance Factor Design for Shallow Transmission Line Structure Foundations. *Journal of Geotechnical and Geoenvironmental Engineering* 129:. [https://doi.org/10.1061/\(asce\)1090-0241\(2003\)129:9\(807\)](https://doi.org/10.1061/(asce)1090-0241(2003)129:9(807))
7. Phoon K-K, Kulhawy FH, Grigoriu MD (2003) Development of a Reliability-Based Design Framework for Transmission Line Structure Foundations. *Journal of Geotechnical and Geoenvironmental Engineering* 129:. [https://doi.org/10.1061/\(asce\)1090-0241\(2003\)129:9\(798\)](https://doi.org/10.1061/(asce)1090-0241(2003)129:9(798))
8. Mukherjee S, Sivakumar Babu GL (2020) Reliability Analysis of Anchor Foundations Subject to Vertical Uplift Forces. *Indian Geotechnical Journal* 50:. <https://doi.org/10.1007/s40098-020-00442-2>
9. Li TZ, Yang XL (2019) An efficient uniform design for Kriging-based response surface method and its application. *Computers and Geotechnics* 109:12–22. <https://doi.org/10.1016/j.compgeo.2019.01.009>
10. Lophaven SN, Nielsen HB, Søndergaard J (2002) DACE: A MATLAB Kriging toolbox
11. ASCE (American Society of Civil Engineers) (2010) *Minimum design loads for buildings and other structures*
12. ASCE (American Society of Civil Engineers) (2009) *Guidelines for Electrical Transmission Line Structural Loading*
13. IS (Indian Standards) (1979) *Code of practice for design and construction of foundations for transmission line towers and poles*. IS 4091. New Delhi, India
14. Baecher GB, Christian JT (2003) *Reliability and Statistics in Geotechnical Engineering*. John Wiley & Sons Ltd, West Sussex, England